Falter, D., Vorogushyn, S., Lhomme, J., Apel, H., Gouldby, B., Merz, B. (2013): Hydraulic model evaluation for large-scale flood risk assessments. - *Hydrological Processes*, *27*, 9, 1331-1340

DOI: 10.1002/hyp.9553

Hydraulic model evaluation for large-scale flood risk assessments

Daniela Falter,[1]* Sergiy Vorogushyn,[1] Julien Lhomme,[2] Heiko Apel,[1] Ben Gouldby[2] and Bruno Merz[1]

1 Deutsches GeoForschungsZentrum GFZ, Sektion 5.4: Hydrologie, Potsdam, Germany
2 HR Wallingford, Howbery Park, Wallingford, Oxfordshire United Kingdom

*Correspondence to: Daniela Falter, Deutsches GeoForschungsZentrum GFZ, Hydrologie, Potsdam, Germany.
E-mail: falter@gfz-potsdam.de

KEY WORDS
model benchmarking; 2D hydraulic models; flood inundation modelling

Abstract

For a nationwide flood risk assessment in Germany, simulations of inundation depth and extent for all major catchments are required. Therefore, a fast two-dimensional hydraulic model is needed. From the range of existing methods, two storage cell models are evaluated to find an appropriate method for large-scale applications. The Dynamic Rapid Flood Spreading Model (Dynamic RFSM) based on irregular storage cells, and a raster-based model with inertia formulation of momentum equation are compared. Simulation performed with the fully dynamic shallow water model InfoWorks RS 2D served as a reference. The hydraulic models are applied to a test area having a very flat topography adjacent to the river Elbe. As a benchmark scenario, the outflow through a hypothetical dike breach was chosen. To investigate the impact of the grid resolution on run time and model performance, the simulation with the raster model is carried out with different grid sizes. Furthermore, the sensitivity of the Dynamic RFSM to the choice of time step was analysed. Both models were able to simulate the final inundation extent and depths with a reasonable accuracy. However, the Dynamic RFSM showed some weakness in simulating inundation extent over the flat test area. Coarsening the grid resolution reduced the run time of the raster-based model considerably and can be regarded as a promising strategy to constrain the computational efforts for a large-scale application, although the model accuracy gradually deteriorated. With similar run time, the raster-based model performed better than the Dynamic RFSM in terms of inundation extent and comparable regarding maximum inundation depth. Generally, an application at national scale appears feasible with both hydraulic modelling schemes.

Introduction

During the last decades, a series of heavy flood events affected Europe and raised the public and scientific interest in flood risk related issues. The assessment of current and future risk and the causes driving the change of risk became important research questions. There is controversy regarding the nature of the trends in flood discharges and their climate drivers

(Wilby et al., 2008; Petrow and Merz, 2009; Villarini et al., 2011). Current research on socio-economic factors indicates that a major contribution to the increase of flood damages in the last decades in Europe seems to be caused by changes in vulnerability (Barredo, 2009).

The European Member States are obliged to carry out flood hazard and risk assessments of each river basin by 2013 as required by the European Directive on Assessment and Management of Flood Risks (EU, 2007). Currently, there appears to be no common strategy or methodological approach among European countries (de Moel et al., 2009). Until recently, relatively few projects have addressed national scale flood risk, e.g. the RASP-project in England and Wales (Hall et al., 2003; Hall et al., 2005) as well as FLORIS-project in the Netherlands (FLORIS, 2005). In Germany, the responsibility of risk assessments is distributed to authorities at the level of federal states (Bundesländer). In most cases, this does not allow a consistent catchment-wide analysis of flood risk. The methodologies used for large-scale flood risk assessments suffer from a number of drawbacks that may constrain the reliability of the results. Risk assessments are typically carried out reach-wise, meaning that an assumption of e.g. a 100-year flood is consecutively applied to each reach based on the extreme value statistics for an upstream gauging station. However, a uniform 100-year event at all gauges is an unrealistic assumption. Such a scenario would lead to the overestimation of flood risk. Another drawback of the reach-wise approach is that the attenuation of a flood wave passing a long and ramified reach is not considered. Floodplain storage, dike overtopping and breaches are therefore not taken into account on a catchment scale, but only considered locally for a particular reach. Wide and flat floodplains in the lowland river parts possess considerable storage capacities that would capture flood peaks and reduce the risk farther downstream. Therefore, continuous unsteady simulations of flow in the whole river network including inundation areas are required.

For a nationwide flood risk assessment in Germany, a complete model chain, starting from rainfall-runoff to damage evaluation is currently being set up. Within this model chain, hydraulic simulations of flood depths and inundation areas will be carried out countrywide for all major river basins including not only main river channels but also tributaries of higher orders. In contrast to other projects, unsteady hydraulic simulations will be performed over long-term periods to investigate the response of flood risk to global changes. Therefore, a fast and efficient hydraulic model for channel flow and floodplain inundation is needed.

For the purposes of hazard assessment, it is widely accepted that river channel flow processes are adequately captured by one-dimensional models. However, inundation processes on a floodplain clearly have a two-dimensional character. Especially in the northern parts of Germany where floodplains are wide and flat, the flood can spread over large areas. For such large-scale applications, usually two-dimensional (2D) models with simplified shallow water equations are applied. The use of the reduced complexity models is often motivated by the intention to reduce computation time, as fully-dynamic 2D models can be very demanding in terms of computational effort. However, the intention to reduce run time by simplification of equations cannot be assumed to be generally valid. This can be concluded from a recent benchmark study of the Environment Agency for England and Wales (UK) (Néelz and Pender, 2010). In that study, the performance of various two-dimensional models from fully-dynamic to very simplified models was investigated. The reduced complexity models were

not always found to be faster than fully-dynamic models. However, the variations between the hardware used to run different codes made it difficult to draw definitive conclusions. On the other hand, Neal et al. (2011a) benchmarked two simplified and one fully-dynamic model within a single code and on a uniform computing platform. They concluded that a simplified diffusive wave model was much slower compared to the recently developed and more complex inertia and the full-dynamic models because of the smaller time steps needed to retain model stability. The straightforward implementations of simplified approaches have the advantage of relatively easy code handling, as opposed to the 2D shallow water equations that need complex numerical solutions and pre-processing steps. Furthermore, reduced complexity approaches are often sufficient to provide the necessary results in terms of accuracy, when compared to the more complex schemes with respect to inundation extent (Horritt and Bates 2001b; Horritt and Bates 2002) and flood risk estimates (Apel et al., 2009).

Among the 2D reduced complexity inundation models, one can further distinguish between models based on continuity and simplified momentum equations, and those based solely on the continuity or floodplain connectivity. Particularly, models based on discretisation of the diffusive wave equation over the 2D Cartesian grids were extensively used in recent years (Bates and de Roo, 2000; Bradbrook et al., 2005; Hunter et al., 2005; Vorogushyn et al., 2010). Their success can be attributed to the relatively simple model structure based on a regular grid and straightforward explicit numerical solutions. The reliance on a regular grid allows a direct use of widely available digital elevation and land-use data for model parameterisation, as well as remote sensing flood extent data for model calibration and validation.

Particularly, the widely used LISFLOOD-FP model (Bates and de Roo, 2000) was successfully applied to a number of catchments, among others to the large-scale basins such as Amazon (Trigg et al., 2009; Wilson et al., 2007) and Ob (Biancamaria et al., 2009). In these studies, the model was applied with a coarse grid resolution to overcome the still high CPU time required. The early LISFLOOD-FP scheme, applied also to the mentioned large scale applications, used a so-called flow limiter approach to counteract numerical instabilities emerging during the computation of flows across cells with deep water and small free surface gradients (Hunter et al., 2005). However, the flow limiter approach suffers from insensitivity of the model to floodplain roughness, which led to the development of an adaptive time step solution scheme for the explicit solver (Hunter et al., 2005). This approach improved the model sensitivity to the roughness parameter, however, at the expense of computational time. Accordingly, the advantage over a fully-dynamical hydraulic model decreased. Driven by this problem, the LISFLOOD-FP code was further developed to include the inertia term into the momentum equation (Bates et al., 2010). With the inclusion of the local acceleration term, the model gained numerical stability. The more stable solution allowed the usage of larger time steps, which positively influenced the computational performance.

Other reduced complexity inundation models are based on the application of the Manning's formula or weir overflow equations on irregular grids. These approaches have a long history, with the first applications dating back to the 1970s (Cunge, 1975) and have experienced a renaissance in the recent years (Moussa and Bocquillon, 2009; Castellarin et al., 2011). The floodplain is represented by interconnected storage cells of irregular shapes. Water volume

fluxes between cells are typically computed by the Manning's equation or weir-type formulas, whereas water levels within the cells are derived from water stage-volume functions. A pre-processing algorithm is needed to define the storage cells and their topology. The definition of the irregular storage cells is often done manually based on distinct topographic features constraining the flood spreading. However, such a subjective delineation may result in an inadequate representation of inundation dynamics. This could especially cause problems in wide and flat areas, where topographic constrains are difficult to evaluate. In the Rapid Flood Spreading Model (RFSM) developed at HR Wallingford (Gouldby et al., 2008), an automatic approach to derive irregular storage cells from a digital elevation model of the floodplain is used. With a search algorithm, local depressions in the topography are located and the storage cells are delineated around them. Hence, this method defines the storage cells in the whole floodplain objectively.

Storage cell models, based on an irregular mesh and using stage-volume functions and simple flux approximations, were developed to perform faster computations when compared to more sophisticated shallow water models. In one respect, this is attributed to the use of very simple equations that do not need complex numerical solution algorithms. Additionally, the fewer number of computational cells reduces the number of calculation steps. Due to representation of sub-grid topography, the water depth variability within the computational cells is retained. The popularity of this approach is probably explained by the need to perform large-scale hydraulic computations. However, these models may suffer from an oversimplified representation of inundation dynamics and may not capture the flood wave propagation properly (e.g. Aureli et al., 2005).

To assess the suitability of simplified hydraulic models for large scale inundation simulations, in this study two models are compared in a benchmarking analysis: the irregular storage cell model Dynamic RFSM (HR Wallingford), based on the diffusive wave approximation, and a raster-based storage cell model with the inertia formulation as proposed by Bates et al. (2010). The objective of this benchmark study is to examine the model efficiency in terms of computational effort as well as the model performance to reproduce the bulk inundation characteristics relevant for large-scale flood risk assessment such as maximum inundation extent and depth. Dynamic RFSM and the raster-based inertia model were part of recent benchmark studies by Néelz and Pender (2010) and Neal et al. (2011a) respectively. This study further complements the two mentioned benchmark studies as Dynamic RFSM and the raster-based inertia model are compared directly. With the intention to evaluate the model performance in lowland areas, where there are few distinct topographic features and flow paths are difficult to identify, a study area in north-eastern Germany was chosen. The area is adjacent to the river Elbe and covers around 2000 km² and was severely affected by flooding in summer 2002. During this event, vast areas of the Elbe floodplain were inundated as a consequence of multiple dike breaches. In the absence of reliable flood event data, such as dike breaches and breach outflows, no real scenario is chosen. Instead a hypothetical dike breach scenario was modelled. Additionally, a simulation with the fully-dynamic shallow water model InfoWorks RS 2D (MWH Soft / Innovyze) was performed and used as a reference for checking the accuracy of the above two model approaches.

In contrast to the regular raster model, the Dynamic RFSM does not have a time step stability constraint, hence the sensitivity of the Dynamic RFSM to time step is also analysed. The choice of time step obviously has a direct influence on the run time; a large time step is desirable as it will reduce the total number of iterations, but a too large time step will produce inaccurate results. Furthermore, the possibility to reduce run time in the raster-based inertia model by coarsening of the grid resolution is examined. Simulations on a raster size from 25 m to 500 m are performed. The accuracy of 2D raster models depending on the grid size were already extensively examined for some test sites, particularly in urban environments (Horritt and Bates, 2001a; Yu and Lane, 2006a; Fewtrell et al., 2008), with the general conclusion that the smoothening of the topography and poorer representation of blockage at coarse grid resolution adversely affects the surface routing processes. However, we particularly test the model performance in terms of run time and accuracy for lowland floodplains typical for eastern-central Germany.

In the following sections, detailed descriptions of the inertia model and the Dynamic RFSM are provided. After performing the comparative analysis, the paper concludes on the applicability of both model types to the countrywide flood risk assessment.

Methods

Raster-based inertia model

In this study a raster-based storage cell model with an implementation of the inertia formulation, as presented by Bates et al. (2010), is used. Thereby the diffusive flood wave formulation is extended by the local acceleration term, whereas the advective acceleration term is still disregarded.

The equation development will be described here briefly, a more detailed derivation is provided by Bates et al. (2010). The inertia model solves the continuity (Eq. 1) and momentum (Eq. 2) equations of the Saint-Venant equations with the latter one neglecting the advective inertial term only:

$$\frac{\partial h^{i,j}}{\partial t} = \frac{q_x^{i-1,j} - q_x^{i,j} + q_y^{i-1,j} - q_y^{i,j}}{\Delta x} \qquad (1)$$

$$\underbrace{\frac{\partial v}{\partial t} + v\frac{\partial v}{\partial x}}_{\text{local and advective acceleration term}} = \underbrace{-g\frac{\partial h}{\partial x}}_{\text{pressure term}} + \underbrace{gS_f}_{\text{friction term}} - \underbrace{gS_0}_{\text{bed slope}} \qquad (2)$$

where, $h^{i,j}$ is the water free surface height, $q^{i,j}$ is the specific flow per unit width at the node (i, j), Δx is the cell dimension, v is velocity, g is gravity, S_f is the friction slope and S_0 is the bed slope.

Expressing the momentum in terms of specific flow per unit width and approximating the hydraulic radius with the flow depth between cells (h_{flow}), the explicit equation for q at time $t+\Delta t$ reads:

$$q_{t+\Delta t} = \frac{q_t - g h_{flow} \Delta t S_f}{(1 + g h_{flow} \Delta t + n^2 |q_t| / h_{flow}^{10/3})} \qquad (3)$$

where n is the Manning's roughness coefficient and Δt is the time step. The fluxes across cell boundaries in x and y directions are computed independently of each other and are used to update the water level using the continuity equation (Eq. 1).

However, the numerical scheme is not unconditionally stable. The time step for a stable numerical solution is constrained by the Courant-Friedrichs-Levy criterion:

$$\Delta t_{max} = \alpha \frac{\Delta x}{\sqrt{g h_{flow}}} \qquad (4)$$

where α was introduced by Bates et al. (2010), as a factor reducing Δt_{max} to enhance model stability. Bates et al. (2010) indicated a value ranging between 0.2 and 0.7 as sufficient for most floodplain flow situations.

The inclusion of the inertia term implies that the water mass can gradually accelerate and decelerate that precludes the flow overshooting and resulting instabilities known for this type of codes (Bates et al., 2010). However, previous studies (Bates et. al, 2010; Dottori and Todini, 2011; Neal et al., 2011b) indicated a small difference between the diffusive storage cell code and the inertia formulation regarding model accuracy. Nevertheless the inertia model requires by far less computational time because of the stabilizing effect of inertia on the numerical solution that allows using larger time steps compared to the diffusive wave approximation. In contrast to the diffusive storage cell code with an adaptive time stepping solution developed by Hunter et al. (2005), the maximum stable time step of the inertia model is 1-3 orders of magnitude larger (Bates et al., 2010). Moreover, with the decreasing cell size, the stable time step of the inertia model reduces linearly instead of quadratic dependence for the diffusive code. This leads to an increased computational performance, especially for fine grid resolutions. Speedups of 2.5 to 1125 times depending on the grid size of 200 m to 5 m were reported for inundation over horizontal planes and planar beaches (Bates et al., 2010).

Dynamic RFSM

The Dynamic Rapid Flood Spreading Model (Dynamic RFSM) is an irregular storage cell model developed by HR Wallingford in 2009. It is based on a previous developed steady-state model, the so-called Direct RFSM (Lhomme et al., 2008; Gouldby et al., 2008). The Direct RFSM determines the final inundation extent by distributing a given water volume over the storage cells. Conversely, the Dynamic RFSM is an unsteady model, which computes fluxes across cell boundaries as a function of time based on the weir formula or Manning's equation. Both Direct and Dynamic RFSM were applied in the model benchmarking exercise conducted by the UK Environment Agency (Néelz and Pender, 2010). That study however, did not

include an inertia based model and did not cover a large scale site of regional extent as is presented here.

The computational mesh of irregular storage cells is established with a fully automated procedure presented in Gouldby et al. (2008). These so called impact zones do not follow a regular raster. Depending on the topography, the impact zones can be very different in size and shape. They are delineated around depressions in the topography. With an automated search algorithm, low points in the digital elevation model (DEM) are identified and denoted as accumulation points (see Fig. 1). Looking at the topography gradient, all DEM cells draining towards the same accumulation point form a polygon called impact zone. All the interfaces between two neighbour impact zones are screened to identify the lowest communication level and the relationship between water level and flow width across the impact zone boundary. Flow between two impact zones is initiated when the water level in one or both impact zones is higher than the communication level. Furthermore, the relationship between water level and storage volume is also calculated for each impact zone. All the information described above characterising the impact zones is stored in a SQL database.

Within the Dynamic RFSM, at each time step, the discharge between the impact zones is calculated with the weir formula or with the Manning's equation using the water levels in the two neighbour impact zones. In this study only the weir formula was used, the model is able to switch automatically between free flow and drowned flow. Water levels are updated using the water depth-volume relationships.

The constant time step at which the calculations are carried out is set by the user. The time step has to be chosen with care. An inappropriate time step may produce inaccurate results, e.g. in a very large time step a high water column can be generated within an impact zone, which in its turn leads to the development of alternative flow pathways across the impact zone boundaries that otherwise would not be activated with small gradual water level increase. This may lead to the development of unrealistic inundation patterns and 'chequerboard' oscillations of the water level. Similar argumentation can be applied to the selection of a very small time step.

InfoWorks

The engine used in the fully-dynamic shallow water model InfoWorks RS 2D (MWH Soft / Innovyze) is based on the procedures described in Alcrudo and Mulet-Marti (2005). It uses a conservative formulation of the full shallow water equations and a first-order finite volume explicit scheme. Fluxes at cell interfaces are calculated with Roe's Riemann Solver. The time step is calculated accordingly to the Courant–Friedrichs–Levy condition. This algorithm can be used with both structured and unstructured meshes and is appropriate for representing rapidly varying flows (shock capturing) as well as super-critical and transcritical flows. Detailed description of the model and a model application can be found respectively in Innovyze (2011) and Lhomme et al. (2010).

Study Area

For the evaluation of both models, a test area adjacent to the river Elbe in Germany was chosen. This reach is part of the middle Elbe and has the characteristics of a lowland river with flat topography and large floodplains. The selected Elbe reach is almost completely protected by dikes.

In Fig. 2, the model domain around the gauge at Torgau is shown. It covers an area of 45 km length and width with a total area of 2025 km². The topographical information is derived from a digital elevation model (DEM) provided by the Federal Agency for Cartography and Geodesy in Germany (BKG, 2007). The DEM was constructed from different information sources, such as digitized topographic maps, photogrammetric and laser scanned data. The horizontal grid resolution is 25 m and the vertical accuracy is reported to be in range of ± 1-5 m. The channel and floodplains between dikes were excluded from the modelling domain (displayed in dark blue in Fig. 2). The inundation simulation over the floodplain in the hinterland was simulated after the initial dike breach was initiated (red circle in Fig. 2).

Floodplain roughness parameters were derived from ATKIS (Amtliches Topographisch-Kartographisches Informationssystem) and CORINE (COoRdinated INformation on the Environment) land-use data by assigning Manning's values to land-use classes. For the mainly agricultural areas, a constant Manning's value of 0.035 $m^{-1/3}s$ is assumed.

Model Testing and Results

For the evaluation of the two models, a hypothetical dike breach scenario along the Elbe reach was implemented. The heavy flood event of August 2002 served as a basis for the calculation of the outflow hydrograph. Water levels within the channel were simulated with a one-dimensional hydraulic model. At the location shown in Fig. 2, a dike breach with a breach width of 20 m was enforced. The outflow from the channel to the floodplain was calculated with the weir formula. The total outflow volume calculated was 55×10^6 m³, distributed over an event duration of 7 days with a maximum outflow of 150 m³/s. However, the total simulated duration was taken as 22 days, to ensure that the steady state was reached. No flow from the floodplain back to the river was considered (i.e. wall boundaries).

Results of the model simulations were evaluated in terms of maximum inundation extent and depth in comparison to a benchmark simulation using the following metrics: bias in depth, root mean square difference (RMSD) of maximum depth, bias in inundated area and flood area index (FAI) defined as follows:

$$FAI = \frac{\mathrm{M1D1}}{\mathrm{M1D1} + \mathrm{M1D0} + \mathrm{M0D1}} \qquad (5)$$

where, M1D1 is the number of cells simulated as flooded by both models, M1D0 is the number of cells flooded in the prediction and dry in the benchmark simulation and M0D1 the number of cells dry in the prediction, however, indicated as wet in the benchmark simulation.

The benchmark is set up with the fully-dynamic shallow water model InfoWorks RS 2D (MWH Soft / Innovyze). Simulations with the raster model and the Dynamic RFSM were performed on a single core only, with an Intel Core Duo 2.66 GHz processor. The InfoWorks simulation was run on two cores at a Pentium 4, 3 GHz CPU. To keep the run time to an acceptable extent, the model domain for the InfoWorks simulations was cut down to the minimum possible extent of 227 km². The computational mesh is made of 234,184 triangles, which have an area comprised between 500 m^2 and 1500 m^2 (i.e. equivalent to square cells of width between 22 m and 39 m). At the given extent, the overall computational time was 64 hours with a minimum time step of 0.058 s. Due to the smaller model domain used and the automatic parallelization on two cores, a direct comparison of run times to Dynamic RFSM and raster-based inertia model should be avoided. The mass balance error was zero.

To be able to compare the benchmark simulation results based on an irregular computational mesh to the results of Dynamic RFSM and raster-based inertia model on regular grids, the benchmark model results were transformed to a regular raster of 5 m resolution. Accordingly, modelling results of the Dynamic RFSM on 25 m and raster-based inertia model on various grid sizes were also resampled to a higher resolution of 5 m. The resampling method used was nearest neighbour. With this method only the resolution, not the value, is changed.

Raster-based inertia model

To investigate the impact of grid resolution on run time and model performance, the two-dimensional simulation with the raster model was repeated several times with different resolutions. Simulations with a grid size varying from 25 m to 500 m were run. The α-value has a direct influence on the model time step and the run time. To find the appropriate α-value, where the solution retains stable while the run time is minimum, an extensive sensitivity analysis would be required for each gird resolution. Furthermore, this analysis would only be valid for this particular test case. However, for large scale and long term applications it is necessary that models are stable for most flow conditions. Therefore, a constant and relatively low α-value of 0.2 was chosen, to guarantee the stability of the solution. Nevertheless for a grid size of 25 m, the water volume spread over the grid was still too large for the time step. Thus, water depths below zero were calculated. Accordingly, the α-value had to be lowered to 0.1 for calculations on a 25 m grid.

A summary of simulation results of the raster model on different grid size, compared to the benchmark, is shown in Table 1. As a comparison between an unstructured and a structured gird is done, one would always find differences in simulation results. However, the smallest difference from the fully-dynamic model simulation in terms of inundation extent and depths was achieved with the finest resolution of 25 m. This difference gradually increases with the grid resolution. In particular the model accuracy significantly deteriorates at a grid resolution of 200 m. There seems to be a local threshold for model accuracy at which the FAI drops by approximately 10% and RMSD increases by ca. 50%. Almost 90% of the flood extent was correctly predicted with the 25 m resolution. The total inundated area is slightly underestimated at 25 m grid size resolution, for coarser grids the total inundated area is generally overestimated as can be concluded from the bias in inundated area.

To illustrate the spatial variation of differences between the benchmark and the inertia based model, the results of the model run with 100 m resolution are shown in Fig. 3. As indicated by the bias and flood area index, the inertia model tends to overestimate the inundation extent as would be expected for coarse resolution, at which topographical boundaries become smoothed. The deviations in depth have been calculated, the absolute error from the reference simulation and the ratio between absolute error and reference depth are shown respectively in Fig. 3 (b) and (c). For the vast majority of the cells in the study area, the absolute error is below 20 cm and the relative error in depth less than 20% of the reference depth given by the benchmark model. High errors in absolute depth (more than 1 m) and relative depth (more than 100%) occur mainly at flood extent boundaries, which can be explained by the discrepancy in simulated inundation areas.

Mass balance errors for the raster-based inertia model were calculated at the end of model simulations as a percentage of the input volume. They remained zero for all simulations, which is a good proxy for model accuracy as recently discussed by Neal et al. (2011a).

For the simulation on the 25 m grid, the run time was approximately 20 days and accordingly almost as long as the actual simulated duration. However, the computational time could be reduced remarkably by coarsening the grid resolution. According to Eq. 4, the time step depends on grid size, flow depth between cells and the α-value. For simulations with a grid resolution up to 200 m, where the difference in modelled depth is small, the minimum time step during the simulation increases linearly with coarsening of the grid. However, this is not valid for the simulation on the 25 m grid, due to the fact that a smaller α-value was necessary to achieve numerical stability. In addition to the increase of minimum time step, the run time is even more reduced by coarsening of the grid resolution and the resulting smaller number of computational elements (Table 1). It can be expected that for larger grid sizes of 100 m and more, larger α-values could be used, which would result in a further reduction of the run time. However, in order to determine the largest α-value at which the model retains stable, a comprehensive and computationally intensive sensitivity analysis for each grid resolution would be required.

Dynamic RFSM

Compared to the regular raster model that runs directly on the DEM, a more extensive pre-processing is needed for the application of the Dynamic RFSM. Firstly, the automatic delineation of impact zones was carried out. The mesh of computational elements was generated from the 25 m resolution digital elevation model (Fig. 4). Around 30,000 impact zones were delineated from around 3 million cells of the digital elevation model. Hence the number of computational elements was reduced by factor 100 compared to a regular raster model for the selected representative lowland floodplain. It can be expected that in other areas with more pronounced relief, the reduction factor is lower if more local topographic depressions are detected. The size and shape of the delineated impact zones varies widely. The mesh of impact zones is shown in Fig. 4. In the very flat areas, some very large impact zones were delineated, with characteristic width of 2 km or more.

The time step within the Dynamic RFSM is constant and set by the user. To test the model sensitivity to the time step size, simulations with time steps of 10 s, 20 s, 40 s, 60 s, 80 s and 100 s were performed with the Dynamic RFSM. The volume exchange between the computational elements was calculated with the weir formula.

During the simulation with a large time step of 100 s, 'chequerboard' type instabilities occurred at locations with high exchange volumes (e.g. close to the breach). Within a single large time step, high water volumes flow from one cell to another, creating temporary high water levels. In the next time step, the water is flowing back into the first cell and so forth. As a result, unrealistic high maximum water depths were calculated. For smaller time steps of 60 s and less, no instabilities could be observed. This type of instability can effectively be suppressed by considering the inertia of water mass as was implemented for the raster-based model (Bates et al., 2010). Initial work on the inclusion of the inertial formulation of the momentum equation within the Dynamic RFSM by Jamieson et al. (2012) gives promising results.

The comparison of the six Dynamic RFSM simulations (Δt = 10, 20, 40, 60, 80, 100 s) with the benchmark results are summarized in Table 2. Overall, the model underestimates the total inundated area as indicated by the bias in inundated area and additionally supported by the low FAI (Table 2). However, the underestimation of maximum inundation depths occurs mainly in areas with very low water depth. As a result, it has a small influence on the RMSD and the depth bias. It appears that, when decreasing the time step the underestimation of inundation extent is increasing. Due to this effect, the decrease of time step from 60 s to 10 s has a negative influence on the RMSD. Although the model runs with 100 and 80 s time steps seem to deliver good results in terms of inundation extent and overall depth bias, the results cannot be used due to the instabilities that occurred during run time producing locally unrealistic high maximum water depth. Therefore, the simulation with a time step of 60 s gives the overall best results in comparison to the fully-dynamic model.

In Fig. 5 (a), showing the 60 s time step simulation compared to benchmark, the underestimation of flood extent becomes evident. In addition it can be seen that a few 'isolated ponds' of inundation were simulated. The large absolute and relative errors in depth up to 0.5 m or 100% respectively, stretching over extended parts of the model domain, are apparent (Fig. 5 (b) and (c)). However, due to the very shallow inundation in these areas, this does not dominate the RMSD value.

For simulations with the Dynamic RFSM, mass balance errors are constrained to zero. This is a result of strict use of discharge limiters implemented. The discharge limiters prevent the total amount of water leaving the cell to be greater than the sum of the initial volume and the volume coming in.

The run times depend roughly linearly on the time step. The simple algorithm, the relatively large time steps and the low number of computational elements enable overall short model run times. However the communications with the SQL database during run time cost a large part of this advantage. The appropriate and structured storage of information is nonetheless

441 indispensable for large-scale applications, where millions of impact zones need to be handled
442 in this framework.

443

444 **Discussion and Conclusion**

445 In the previous sections, two simplified hydraulic models, an inertia based raster model and
446 the Dynamic RFSM, were compared to a benchmark scenario. The objective was to
447 investigate their ability to simulate a hypothetical inundation scenario, in comparison to the
448 fully-dynamic InfoWorks model. The accomplished tests included a sensitivity analysis of the
449 raster model to grid size and of the Dynamic RFSM to time step, with respect to model
450 accuracy and run time.

451 Simulations of inundation processes in the selected lowland study area with wide and flat
452 floodplains were shown to be specifically challenging because of multiple possible flow
453 paths. The simulated scenarios have shown that both simplified models were able to simulate
454 the final inundation extent and depths with a reasonable accuracy.

455 As was expected, the raster-based model delivered the best results at the finest tested grid
456 resolution of 25 m corresponding to the original DEM resolution used for the benchmark
457 model. However, the total computational time at this resolution becomes intractable in view
458 of the national scale application. Much progress has been made over the past decade with
459 raster-based models to develop simplified and fast hydrodynamic schemes. However they still
460 remain CPU time demanding for large scale problems. Therefore, the strategy of grid
461 coarsening has to be taken into account to cope with computational constraints. It was shown
462 that the model accuracy deteriorates with increasing grid size, as one would have expected,
463 when the topographic constraints become smoothed by interpolation. Indeed, the inertia
464 model tends to overestimate the inundation extent at coarser grids compared to the benchmark
465 result. It is however, evident that doubling the cell size results in a considerable decrease of
466 computational time. Although one must keep the acceptable accuracy level for hydraulic
467 simulations, this does not seem to dominate the risk estimations (Apel et al., 2009), which is
468 especially true for large scale applications, where the local errors can counteract each other in
469 the final risk estimate.

470 Even with its simplified structure that uses a diffusive-wave approximation on an irregular
471 grid, the Dynamic RFSM was able to simulate the maximum inundation extent and depths in
472 a reasonable manner, although problems occurred with very large impact zones delineated in
473 the flat regions of the case study area. Isolated ponds of inundation were simulated in the
474 study area. This effect is caused by the filling of the impact zones that starts from the lowest
475 point. Whenever an impact zone is not completely filled, the crest between the considered
476 impact zone and its neighbours is not inundated. This effect increases with larger inundation
477 zones and leads to a marked underestimation of inundation extent in the affected areas.
478 However, as indicated by the RMSD, the overall maximum depth is in generally well-
479 reproduced, due to the fact that these effects only occur in areas with very shallow inundation.
480 These problems are likely to be less dominant in areas with a complex topography where
481 generally smaller inundation zones are delineated. Care has to be taken with the choice of

time step, as it affects model performance. At large time steps, the level in a given impact zone is likely to rise too high as the exchanged volume was too high. This impact zone will be able to spill towards more neighbours compared to the case where the level is properly estimated. For a too large time step of 100 s 'chequerboard' type of instabilities could be observed. With a shorter time step, the level is likely to rise to a more moderate value and potentially fewer neighbours will be spilt into. A time step of 60 s was optimal in this study area for impact zones of the given size. This type of instability can effectively be suppressed by the implementation of the inertial type approach (Bates et al., 2010). Early exploration of the inclusion of the local acceleration term of the momentum equation within the formulation of the Dynamic RFSM shows considerable promise (Jamieson et al., 2012).

Using a relatively coarse grid resolution of 100 m can reduce the run time of the raster-based model to the run time similar to the computational time of the Dynamic RFSM with a time step of 60 s (Table 1 and 2). Comparing the results, the raster based model performs better than the Dynamic RFSM in terms of inundation extent, as indicated by FAI and bias in inundated area. On the contrary, the Dynamic RFSM achieved a slightly better RMSD compared to the benchmark simulation. This is an advantage of the Dynamic RFSM over the current version of the inertia model which basically resides in consideration of the sub-grid topographic variability within the impact zones. This characteristic is crucial for representing the inundation depths. On a coarse grid the inertia model uses the averaged topography, whereas Dynamic RFSM retains the detailed topographic information within each impact zone. The advanced model physics in the inertia model cannot fully compensate the reduction in topographic complexity with respect to the simulation of inundation depths.

Thus, overall it can be concluded that with a similar run time, the raster-based model performs slightly better than the Dynamic RFSM in this lowland river case study. Furthermore, there is a potential for reduction of run times of the inertia model by using higher α-values for larger grid sizes. Determination of the highest possible α-value at which the model retains stability requires, however, a computationally intensive sensitivity analysis. An additional advantage of the raster-based model is the easier model set up which does not require additional pre-processing steps. Nevertheless, it is likely that in areas with more complex topography, the generalization of the DEM has more influence on modelling results. It is possible, that in this case the raster based model might fail to simulate the inundation process correctly on a coarse grid resolution. This problem can however, be relaxed by the implementation of the sub-grid parameterisation schemes aimed at the representation of influences on flow conveyance by small-scale topographical features at a larger scale. This can be realized by deriving a so-called porosity function on a cell basis, which accounts for flow blocking effects by topographic features (e.g. buildings), reduction in floodplain storage and alteration in flow pathways (Defina, 2000; Yu and Lane, 2006b; McMillan and Brasington, 2007; Soares-Frazao et al., 2008). For instance, for the raster cell models, a porosity function can be implemented as a depth dependent percentage of volume of a coarse resolution cell available for storage (Yu and Lane, 2006b; McMillan and Brasington, 2007). In this approach, the sub-grid topographic variability is represented by the volume-depth relationships on a grid-by-grid basis, and is in essence the one used in RFSM models for irregular cells. The porosity models were reported to resemble the hydrodynamics of the high-

resolution flow models, however, the improvement obviously comes at the expense of computational time (Yu and Lane, 2006b; McMillan and Brasington, 2007).

Previous application of the Dynamic RFSM model revealed some difficulties in the propagation of high flows (Néelz and Pender, 2010). However this was mainly the result of using too large time steps in order to achieve short run times. This is a common problem with diffusion wave models with no adaptive time stepping (Hunter et al., 2005). This situation has given an impetus to a further development of the Dynamic RFSM model and early work on an adaptation of the inertial form of the momentum equation to the irregular polygon structure shows great potential. This benchmark exercise is, however, particularly focused on the flood characteristics relevant for inundation risk assessment such as maximum inundation extent and depths. With regards to these characteristics, the Dynamic RFSM performed satisfactorily in the present test.

Hence, an application at the national scale appears feasible with both the Dynamic RFSM and the inertia model as they showed reasonable run times and acceptable performance.

Acknowledgements

The work reported in this paper is part of the project “Regional Flood Model for Germany”. We thank the Federal Agency for Cartography and Geodesy in Germany (BKG) for provision of the digital elevation model of Germany (DGM-D) and the two anonymous reviewers for their helpful comments and suggestions.

References

Alcrudo F, Mulet-Marti J. 2005. Urban inundation models based upon the shallow water equations. Numerical and practical issues. In: F. Benkhaldoun, D. Ouazar, S. Raghay, eds. *Proceedings of finite volumes for complex applications IV. Problems and perspectives*. Hermes Science, 1–12.

Apel H, Aronica GT, Kreibich H, Thieken AH. 2009. Flood risk analyses - how detailed do we need to be? *Natural Hazards*, **49**: 79-98.

Aureli F, Maranzoni A, Mignosa P, Ziveri C. 2005. Flood hazard mapping by means of fully-2D and quasi-2D numerical modelling: a case study. In: Alphen V, van Beek, Taal (Eds.), *Floods, from defence to management*. Taylor & Francis Group, London, 41–51.

Barredo JI. 2009. Normalised flood losses in Europe: 1970–2006. *Natural Hazards and Earth System Sciences*, **9**: 97-104.

Bates PD, De Roo APJ. 2000. A simple raster-based model for flood inundation simulation. *Journal of Hydrology* , **236**: 54-77.

Bates PD, Horritt MS, Fewtrell TJ. 2010. A simple inertial formulation of the shallow water equations for efficient two-dimensional flood inundation modelling. *Journal of Hydrology*, **387**: 33-45.

Biancamaria S, Bates PD, Boone A, Mognard NM. 2009. Large-scale coupled hydrologic and hydraulic modelling of the Ob river in Siberia. *Journal of Hydrology*, **379**: 136-150.

BKG. 2007. Digitales Geländemodell für Deutschland DGM-D, technical report, Frankfurt am Main, Germany. (Available at http://www.geodatenzentrum.de/docpdf/dgm-d.pdf)

567 Bradbrook K, Waller S, Morris D. 2005. National Floodplain Mapping: Datasets and Methods
568 - 160,000 km in 12 month. *Natural Hazards, **36***: 103-123.
569 Castellarin A, Domeneghetti A, Brath A. 2011. Identifying robust large-scale flood risk
570 mitigation strategies: A quasi-2D hydraulic model as a tool for the Po river. *Physics and*
571 *Chemistry of the Earth,* **36**: 299–308.
572 Cunge JA. 1975. Two-dimensional modeling of flood plains. *Water Resources Publications*,
573 Ch. 17: 705–762.
574 Defina A. 2000. Two-dimensional shallow flow equations for partially dry areas. *Water*
575 *Resources Research*, **36**: 3251-3264.
576 Dottori F, Todini E. 2011. Developments of a flood inundation model based on the cellular
577 automata approach: Testing different methods to improve model performance. *Physics and*
578 *Chemistry of the Earth,* **36**: 266-280.
579 EU. 2007. Directive 2007/60/EC of the European Parliament and of the Council of 23
580 October 2007 on the assessment and management of flood risks. *Journal of the European*
581 *Union,* **L228**: 27–34.
582 Fewtrell TJ, Bates PD, Horritt M, Hunter NM. 2008. Evaluating the effect of scale in flood
583 inundation modelling in urban environments. *Hydrological Processes,* **22**: 5107-5118.
584 FLORIS. 2005. Flood Risks and Safety in the Netherlands (Floris). Floris study - Full report,
585 Ministerie van Verkeer en Waterstaat, DWW-2006-014, ISBN 90-369-5604-9.
586 Gouldby B, Sayers P, Mulet-Marti J, Hassan M, Benwell D. 2008. A methodology for
587 regional-scale flood risk assessment. *Proceedings of the Institution of Civil Engineers -*
588 *Water Management,* **161**: 169-182.
589 Hall JW, Dawson RJ, Sayers PB, Rosu C, Chatterton JB, Deakin R. 2003. A methodology for
590 national-scale flood risk assessment. *Proceedings of the Institution of Civil Engineers,*
591 *Water & Maritime Engineering,* **156**: 235-247.
592 Hall JW, Sayers PB, Dawson RJ. 2005. National-scale Assessment of Current and Future
593 Flood Risk in England and Wales. *Natural Hazards,* **36**: 147-164.
594 Horritt MS, Bates PD. 2001a. Effects of spatial resolution on a raster based model of
595 floodplain flow. *Journal of Hydrology,* **253**: 239–249.
596 Horritt MS, Bates PD. 2001b. Predicting floodplain inundation: raster-based modelling versus
597 the finite-element approach. *Hydrological Processes,* **15**: 825-842.
598 Horritt MS, Bates PD. 2002. Evaluation of 1D and 2D numerical models for predicting river
599 flood inundation. *Journal of Hydrology,* **268**: 87-99.
600 Hunter NM, Horritt MS, Bates PD, Wilson MD, Werner MGF. 2005. An adaptive time step
601 solution for raster-based storage cell modelling of floodplain inundation. *Advances in*
602 *Water Resources,* **28**: 975-991.
603 Innovyze. 2011. *Infoworks 11.5 RS Help*. Wallingford: Innovyze.
604 Lhomme J, Sayers P, Gouldby B, Samuels P, Wills M. 2008. Recent development and
605 application of a rapid flood spreading method. In: P. Samuels et al., ed. 2008. *Flood risk*
606 *management: research and practice*. Taylor & Francis Group, London, UK.
607 Jamieson S, Wright G, Lhomme, J and Gouldby B. 2012. Validation of a Computationally
608 Efficient 2D Inundation Model on Multiple Scales. *Floodrisk 2012*, Rotterdam, Taylor &
609 Francis Group, *in press*.

610 Lhomme J, Gutierrez-Andres J, Weisgerber A, Davison M, Mulet-Marti J, Cooper A,
611 Gouldby B. 2010. Testing a new two-dimensional flood modelling system: analytical tests
612 and application to a flood event. *Journal of Flood Risk Management,* **3**: 33-51.
613 McMillan H, Brasington, J. 2007. Reduced complexity strategies for modelling urban
614 floodplain inundation. *Geomorphology*, **90**: 226-243.
615 de Moel H, van Alphen J, Aerts JCJH. 2009. Flood maps in Europe - methods, availability
616 and use. *Natural Hazards and Earth System Sciences ,* **9**: 289-301.
617 Moussa R, Bocquillon C. 2009. On the use of the diffusive wave for modelling extreme flood
618 events with overbank flow in the floodplain. *Journal of Hydrology,* **374**: 116–135.
619 Neal J, Villanueva I, Wright N, Willis T, Fewtrell T, Bates P. 2011a. How much physical
620 complexity is needed to model flood inundation? *Hydrological Processes,*
621 DOI: 10.1002/hyp.8339.
622 Neal J, Schumann G, Fewtrell T, Budimir M, Bates PD, Mason D. 2011b. Evaluating a new
623 LISFLOOD-FP formulation with data from the summer 2007 foods inTewkesbury,UK.
624 *Journal of Flood Risk Management,* **4**: 88–95.
625 Néelz S, Pender G. 2010. Benchmarking of 2D hydraulic modelling packages. Bristol, UK:
626 Environment Agency.
627 Petrow T, Merz B. 2009. Trends in flood magnitude, frequency and seasonality in Germany in
628 the period 1951–2002. *Journal of Hydrology,* **371**: 129-141.
629 Soares-Frazao S, Lhomme J, Guinot V, Zech Y. 2008. Two-dimensional shallow water
630 models with porosity for urban flood modelling. *Journal of Hydraulic Research,* **46**: 45-64.
631 Trigg MA, Wilson MD, Bates PD, Horritt MS, Alsdorf DE, Forsberg BR, Vega MC. 2009.
632 Amazon flood wave hydraulics. *Journal of Hydrology,* **374**: 92-105.
633 Villarini G, Smith JA, Serinaldi F, Ntelekos AA. 2011. Analyses of seasonal and annual
634 maximum daily discharge records for central Europe. *Journal of Hydrology,* **399**: 299-312.
635 Vorogushyn S, Merz B, Lindenschmidt K-E, Apel H. 2010. A new methodology for flood
636 hazard assessment considering dike breaches. *Water Resources Research,* **46:** W08541.
637 Wilby RL, Beven KJ, Reynard NS. 2008. Climate Change and fluvial flood risk in the UK:
638 more of the same? *Hydrological Processes,* **22**: 2511-2523.
639 Wilson M, Bates P, Alsdorf D, Forsberg B, Horritt M, Melack J, Frappart F, Famiglietti J.
640 2007. Modeling large-scale inundation of Amazonian seasonally flooded wetlands.
641 *Geophysical Research Letters,* **34**: L15404.
642 Yu D, Lane SN. 2006a. Urban fluvial flood modelling using a two-dimensional diffusion-
643 wave treatment, part 1: mesh resolution effects. *Hydrological Processes,* **20**: 1541-1565.
644 Yu D, Lane SN. 2006b. Urban fluvial flood modelling using a two-dimensional diffusion-
645 wave treatment, part 2: development of a sub-grid-scale treatment. *Hydrological*
646 *Processes,* **20**: 1567-1583.
647

648

649

650

Tables

Table 1: Influence of grid resolution on maximum simulated inundation extent and depth, as well as on run time, for simulations with the raster-based inertia model.

Grid resolution	Bias in depth (m)	RMSD (m)	Bias in inundated area	Flood area index (%)	Number of computational cells	Minimum occurred time step (s)	Run times (min)
25 m	-0.02	0.14	0.98	89.0	3,097,600	0.4	27,840
50 m	-0.006	0.16	1.02	89.6	774,400	1.6	1,555
100 m	+0.0006	0.21	1.05	86.9	193,600	3.3	154
200 m	+0.01	0.34	1.13	75.7	48,400	6.8	21.6
300 m	+0.02	0.40	1.18	70.8	21,609	7.3	7.3
400 m	+0.006	0.43	1.19	68.9	12,100	9.2	4.5
500 m	+0.004	0.49	1.08	57.0	7,744	12.9	3.4

Table 2: Influence of time step on maximum simulated inundation extent and depth, as well as on run time, for simulations with the Dynamic RFSM.

Time step size	Bias in depth (m)	RMSD (m)	Bias in inundated area	Flood area index (%)	Run times (min)
10 s	-0.09	0.19	0.76	73.5	558
20 s	-0.08	0.18	0.78	75.0	289
40 s	-0.05	0.17	0.81	76.9	147
60 s	-0.03	0.17	0.83	78.0	102
80 s	-0.01	0.19	0.86	79.0	79
100 s	+0.007	0.22	0.88	79.1	64

700 **Figures**

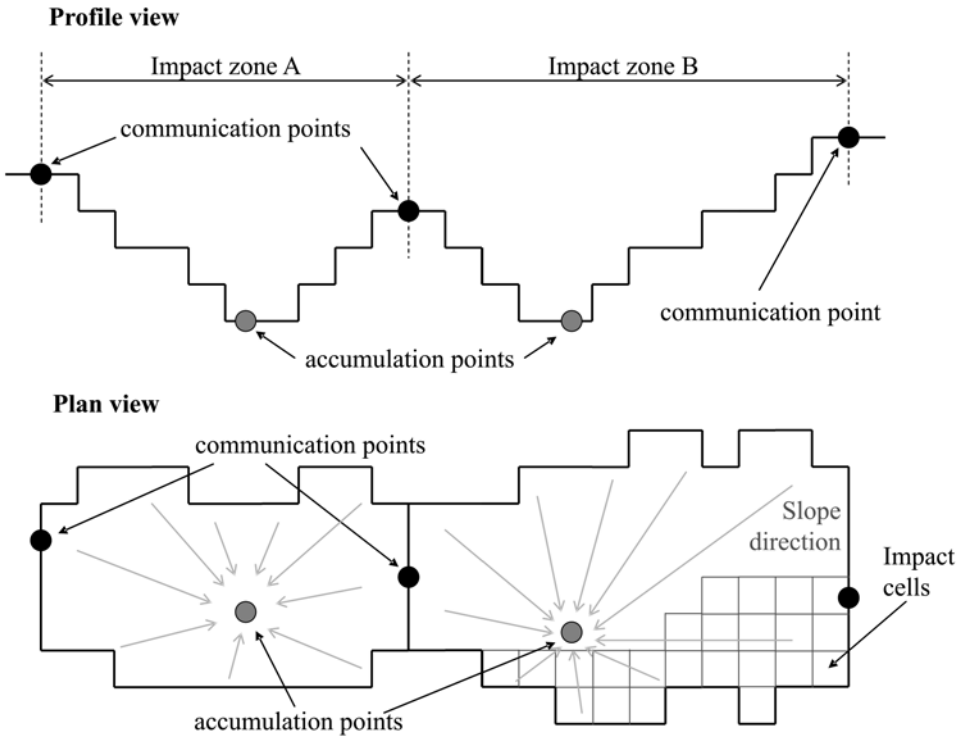

701

702 Figure 1. Example structure of impact zones (Lhomme et al., 2008)

703

704

705

706

707

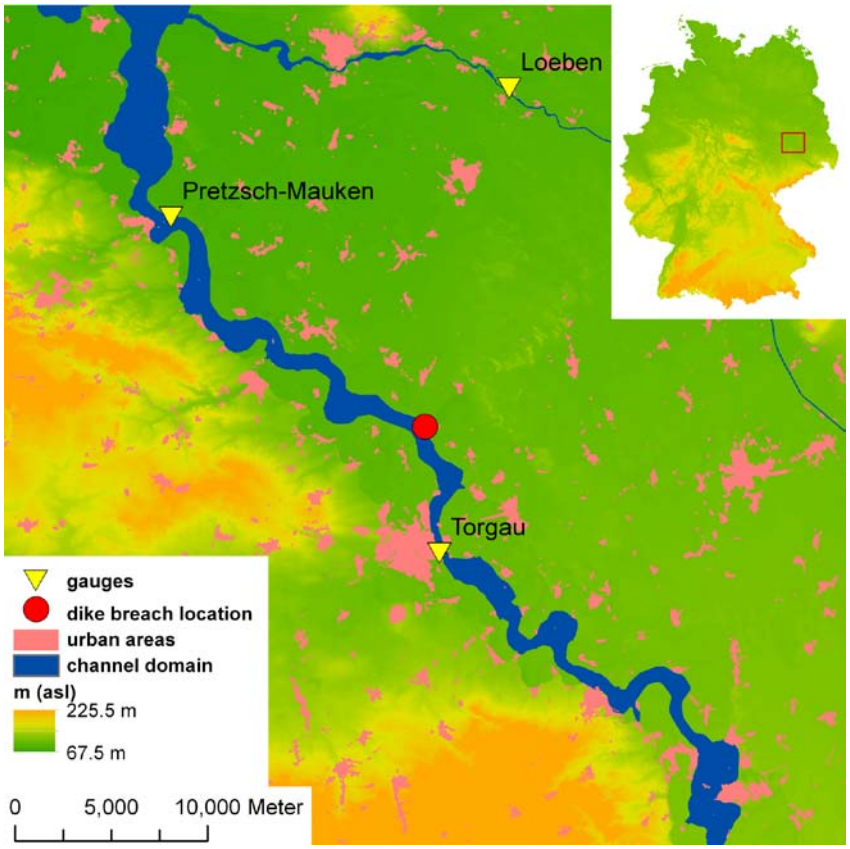

Figure 2. Model domain of the study area at the river Elbe

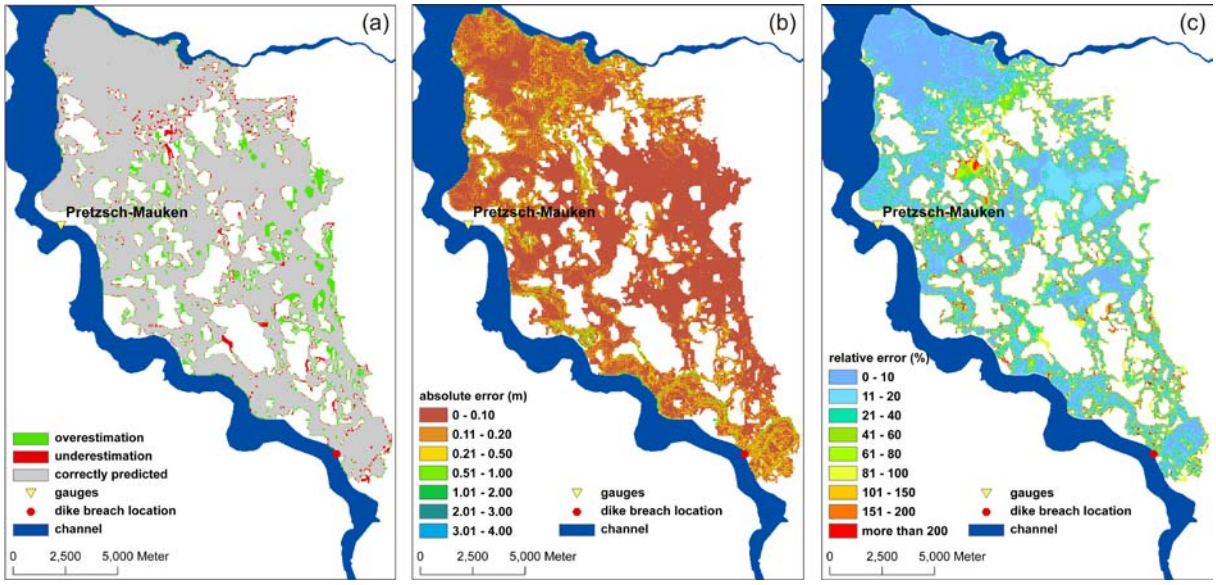

Figure 3. Comparison of maximum simulated inundation depths between the raster-based model simulation (at Δx = 100 m) and benchmark. (a) Evaluation of inundation extent, (b) absolute error in depth, (c) ratio between absolute error and reference depth

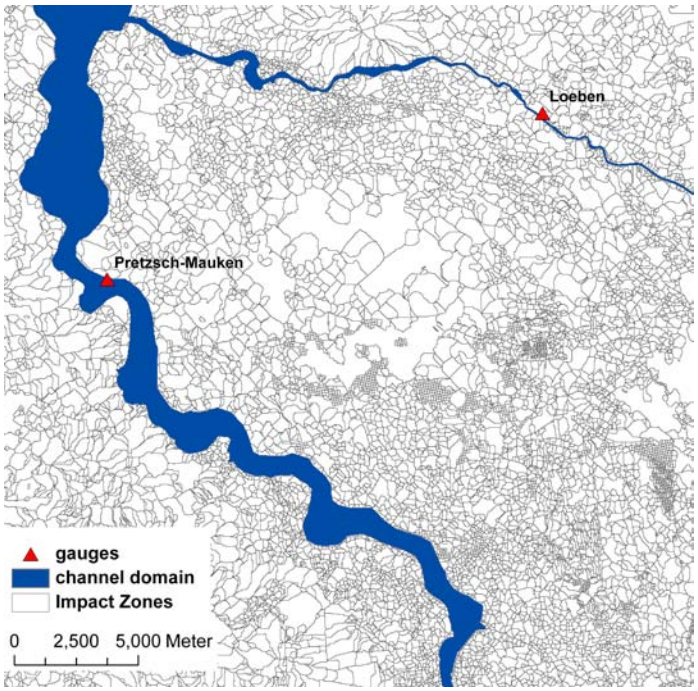

Figure 4. Mesh of impact zones within the modelling domain

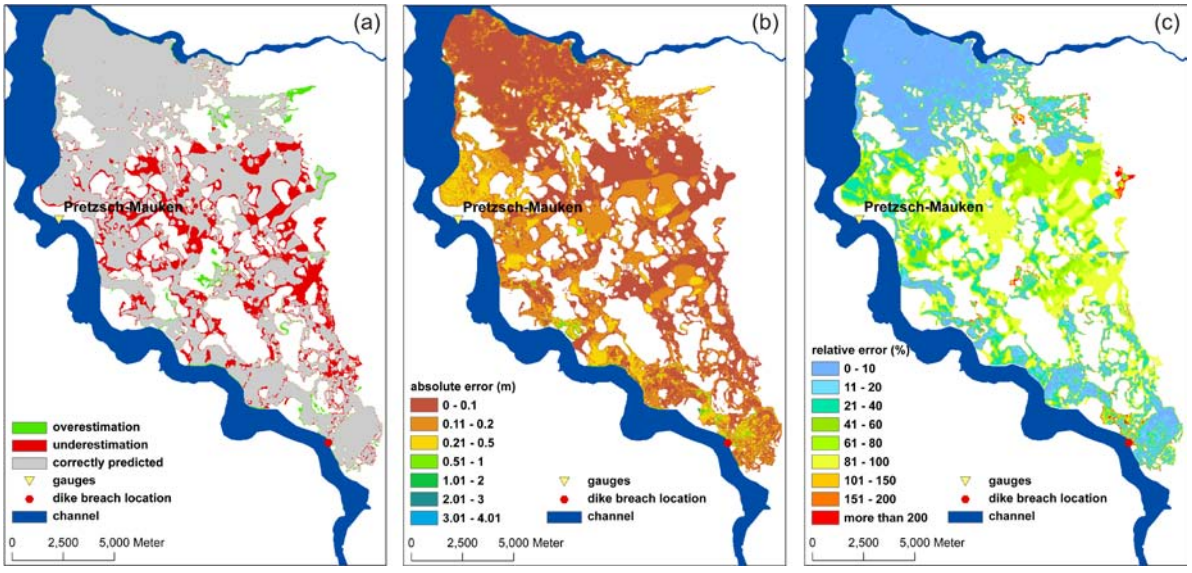

Figure 5. Comparison of maximum simulated inundation depths between Dynamic RFSM simulation (with Δt = 60 s) and benchmark. (a) Evaluation of inundation extent, (b) absolute error in depth, (c) ratio between absolute error and reference depth